

Predicting relapse in medulloblastoma patients by integrating evidence from clinical and genomic features

Tamayo et al

Data Supplement

Table S1. Clinical characteristics of patients in the training and test datasets.

Table S2. Disease-subtype expression signatures used to predict disease-subtype in the test set.

Figure S1. Kaplan-Meier survival plots and ROC curves for the Pomeroy et al. 2002 signature in the training and test sets.

Figure S2. Set of 36 expression signatures used to predict disease-subtype in test samples. Six expression signatures were chosen from the top 10 according to the au-ROC scores for each disease-subtype $\{c_1, \dots, c_6\}$.

Figure S3. Heat map of the top 20 disease-independent expression signatures that discriminate relapse vs. no-relapse according to the au-ROC in the training dataset. We selected c-Myc as the representative disease-independent expression signatures to be used in the model.

Figure S4. Heat map of the top 20 (bottom 20) disease-dependent pathways that discriminate relapse vs. no-relapse according to the au-ROC for each disease-subtype $\{c_1, \dots, c_6\}$ in the training dataset. The boxes show the ones we selected to be representative of disease-independent expression signatures to be used in the model.

Figure S5. Kaplan-Meier plots and log-rank test p-values of the associated rank test for the current clinical schema and Models A-D in: A) the training set, and B) the test set. The 95% confidence intervals are shown in blue.

Figure S6. Relative utility curves for Models A-D in the training and test sets. The plots show the relative utility, i.e., the fraction of the utility of perfect prediction that is achieved at the optimal cut point for a risk prediction model, vs. risk threshold. We note that the curves for Models C and D overlap for both the train and test sets.

Figure S7. Full Bayesian nomogram showing all the arms corresponding to disease-subtype dependent expression signatures conditional to the disease-subtype. A specific instance of this nomogram populated with the features of one patient is shown on Fig 3.

Figure S8. Flow-chart of the entire model methodology showing the steps that have to be performed for the analysis of training and test samples. The orange and pink squares represent experimental procedures, and the blue squares represent computational steps. The green squares represent datasets or computational models.

TABLE S1

Attribute	Training Dataset	Test Dataset
Number of Samples	96	78
Sex		
Female	38.5%	30.8%
Male	61.5%	69.2%
Relapse		
No	57.3%	56.4%
Yes	42.7%	43.6%
Status		
Alive	67.7%	66.7%
Deceased	30.2%	33.3%
Unknown	2.1%	-
Average Age (months)	107.4 ± 69.9	105.6 ± 88.3
Histology		
Classic	67.7%	71.8%
Desmoplastic	13.5%	17.9%
LGA (Large Cell Anaplastic)	16.7%	-
Unknown	2.10%	10.3%
Metastasis		
M0	75.0%	66.7%
M1	3.12%	8.97%
M2	2.08%	2.56%
M3	9.38%	12.8%
M4	-	2.18%
M+	2.08%	2.56%
Unknown	8.33%	-
Risk		
Standard	60.4%	65.3%
High	30.2%	28.2%
Unknown	9.40%	6.5%

TABLE S2

Feature	Subtype	Description	Database
Expression Signatures Used to Predict Disease-Subtype			
TRANSLATION_FACTORS	C ₁	Translation factor genes (52) GenMAPP	MSigDB v2.5/C2
BRCA_BRCA1_POS	C ₁	Genes whose expression is consistently positively correlated with brca1 germline status (107)	MSigDB v2.5/C2
FLUMAZENILPATHWAY	C ₁	Flumazenil pathway (9 genes)	MSigDB v2.5/C2
AGUIRRE_PANCREAS_CHR8	C ₁	Genes (61) on chr with copy-number-driven expression in pancreatic adenocarcinoma.	MSigDB v2.5/C2
MENSSEN_MYC_UP	C ₁	Genes (34) up-regulated by MYC in HUVEC (umbilical vein endothelial cell)	MSigDB v2.5/C2
PENG_RAPAMYCIN_DN	C ₁	Genes (229) downregulated in response to rapamycin starvation	MSigDB v2.5/C2
DSRNA_UP/DN	C ₂	Upregulated (38) and downregulated (15) by dsRNA (polyI:C) in IFN-null GRE cells	MSigDB v2.5/C2
HINATA_NFKB_DN	C ₂	Genes (25) downregulated by NF-kappa B	MSigDB v2.5/C2
P53_DN.v2	C ₂	Genes upregulated (150) and downregulated (150) in siRNA knockdown of p53 (GEO dataset GDS1852).	OPAM.v3
IL22BPPATHWAY	C ₂	IL-22 (13) is produced by T cells and induces the acute phase inflammatory response in hepatocytes.	MSigDB v2.5/C2
ABBUD_LIF_GH3_DN	C ₂	Genes (7) that decreased after LIF treatment of GH3 cells	MSigDB v2.5/C2
NGUYEN_KERATO	C ₂	Genes concomitantly upregulated (29) and downregulated (86) by activated Notch1 in mouse and human primary keratinocytes	MSigDB v2.5/C2
POMEROY_DESMOPLASIC_VS_CLASSIC_MD_UP	C ₃	Genes (47) expressed in desmoplastic medulloblastomas.	MSigDB v2.5/C2
HSA04340_HEDGEHOG_SIGNALING_PATHWAY	C ₃	Genes (57) involved in Hedgehog signaling pathway	MSigDB v2.5/C2
HINATA_NFKB	C ₃	Genes upregulated (111) and downregulated (21) by NF-kappa B	MSigDB v2.5/C2
RADAEVA_IFNA_DN	C ₃	Genes (10) down-regulated by interferon-alpha in primary hepatocyte	MSigDB v2.5/C2
RORIE_ES_PNET_UP	C ₃	Genes (28) showing the greatest increase in expression in NBa Ews/Fli-1 infantants	MSigDB v2.5/C2
SARCOMAS_LIPOSARCOMA	C ₃	Genes upregulated (10) and downregulated (11) in liposarcomas, versus other soft-tissue tumors.	MSigDB v2.5/C2
GPCRS_CLASS_C_METABOTROPIC_Glutamate_PHEROMONE	C ₄	Genes (14) associated with G-protein coupled receptors related to metabotropic glutamate receptors.	MSigDB v2.5/C2
DFOSB_BRAIN_2WKS_UP	C ₄	Genes (39) Up-regulated in nucleus accumbens of mice after 2 weeks of induction of transgenic deltaFosB	MSigDB v2.5/C2
PARKINPATHWAY	C ₄	Genes (12) associated with Parkinson's disease	MSigDB v2.5/C2
HSA05020_PARKINSONS_DISEASE	C ₄	Genes (17) involved in Parkinson's disease	MSigDB v2.5/C2
MITRPATHWAY	C ₄	Genes (9) associated with the MyoD/MEF2 transcription factors	MSigDB v2.5/C2
HSA04080_NEUROACTIVE_LIGAND_RECEPTOR_INTERACTION	C ₄	Genes (254) involved in neuroactive ligand-receptor interaction	MSigDB v2.5/C2
PHOTO_DN.v1	C ₅	Photoreceptor upregulated (150) and downregulated (150) genes (Cepko et al. 2007 ¹)	OPAM.v3
CRX_DN.v1	C ₅	CRX -/- upregulated (150) and downregulated (150) genes (Cepko et al. 2007 ¹)	OPAM.v3
CtIP_DN.v1	C ₅	CtIP -/- upregulated (150) and downregulated (150) genes (GEO dataset GDS2189)	OPAM.v3
NRL_DN.v1	C ₅	NRL -/- upregulated (150) and downregulated (150) genes (Cepko et al. 2007 ¹)	OPAM.v3
WNT_UP.v1	C ₅	Genes upregulated (200) and downregulated (200) by wnt (GEO dataset GSE1899).	OPAM.v3
CHREBPPATHWAY	C ₅	Genes (20) associated with chREBP, a transcription factor inhibited by cAMP	MSigDB v2.5/C2
NEUROTRANSMITTERSPATHWAY	C ₆	Genes (6) associated with biosynthesis of neurotransmitters	MSigDB v2.5/C2
BCAT_UP.v1_UP	C ₆	Genes (200) upregulated by beta-catenin (GEO dataset GDS748)	OPAM.v3
ST_WNT_BETA_CATENIN_PATHWAY	C ₆	Genes (34) associated with Wnt/Beta-catenin signaling.	MSigDB v2.5/C2
LEF1_UP.v1_UP	C ₆	Genes (200) upregulated by Lef1 (GEO dataset GSE3229)	OPAM.v3
TGFBETA_LATE_UP	C ₆	Genes (33) upregulated by TGF-beta treatment of skin fibroblasts only at 1-4 hrs (clusters 4-6)	MSigDB v2.5/C2
UVB_NHEK3_C6	C ₆	Genes (30) regulated by UV-B light in normal human epidermal keratinocytes, cluster 6	MSigDB v2.5/C2

1. Corbo JC, Myers CA, Lawrence KA, et al: A typology of photoreceptor gene expression patterns in the mouse. Proc Natl Acad Sci U S A 104:12069-74, 2007

Figure S1

Pomeroy et al. 2002 8-gene outcome signature

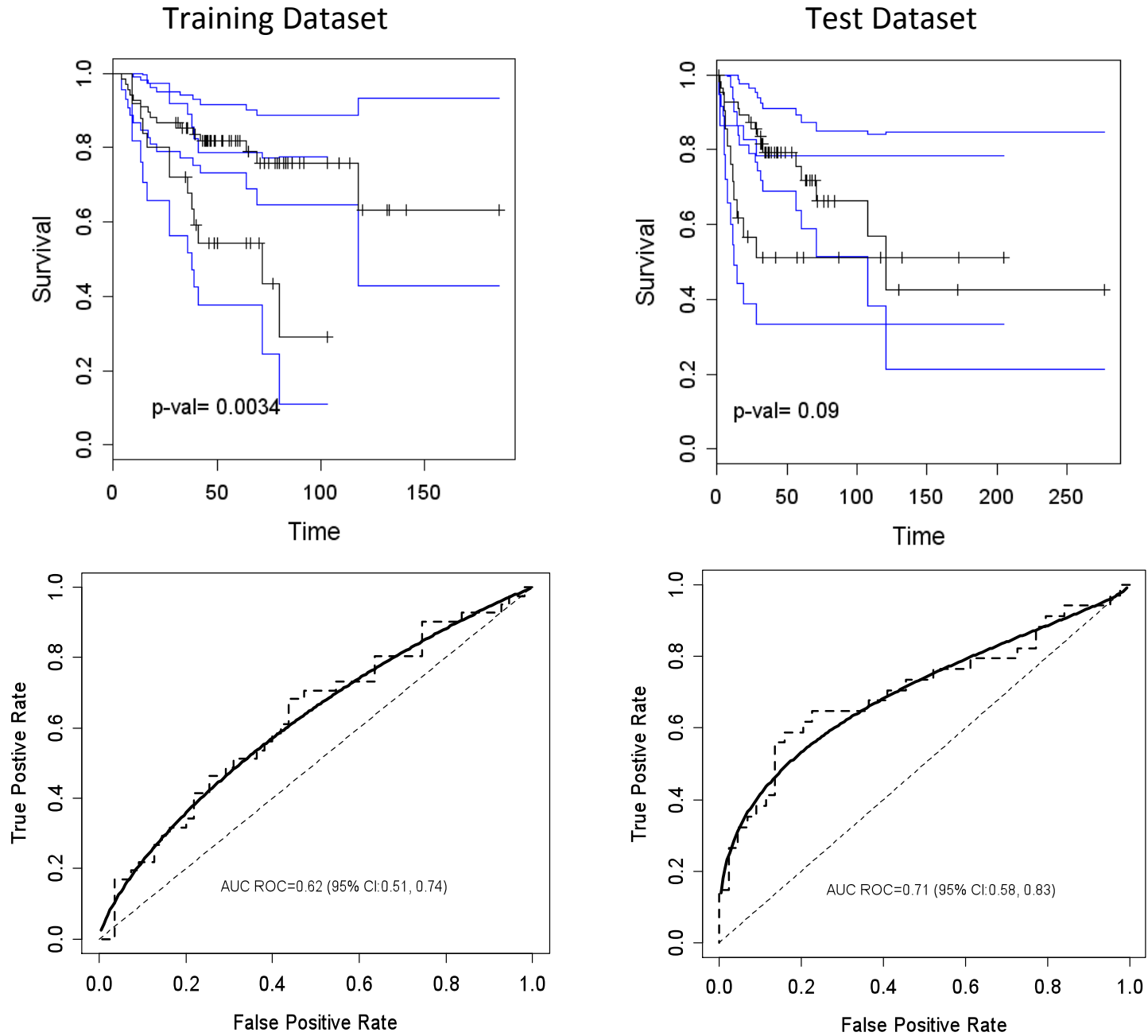


Figure S2

Expression Signatures that Predict Disease-Subtype - Training Set

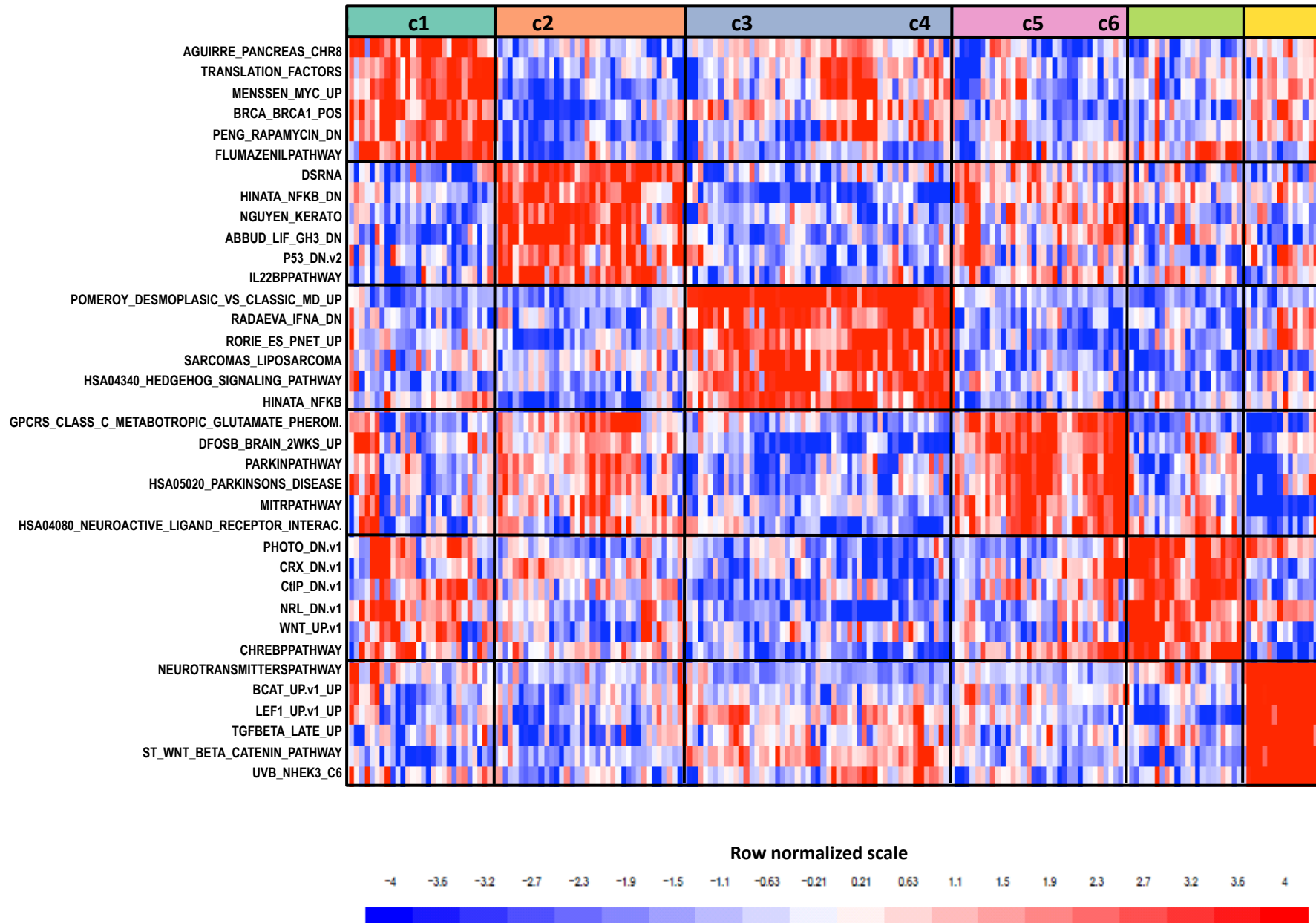


Figure S3

Disease-Subtype Independent Expression Signature Training Set

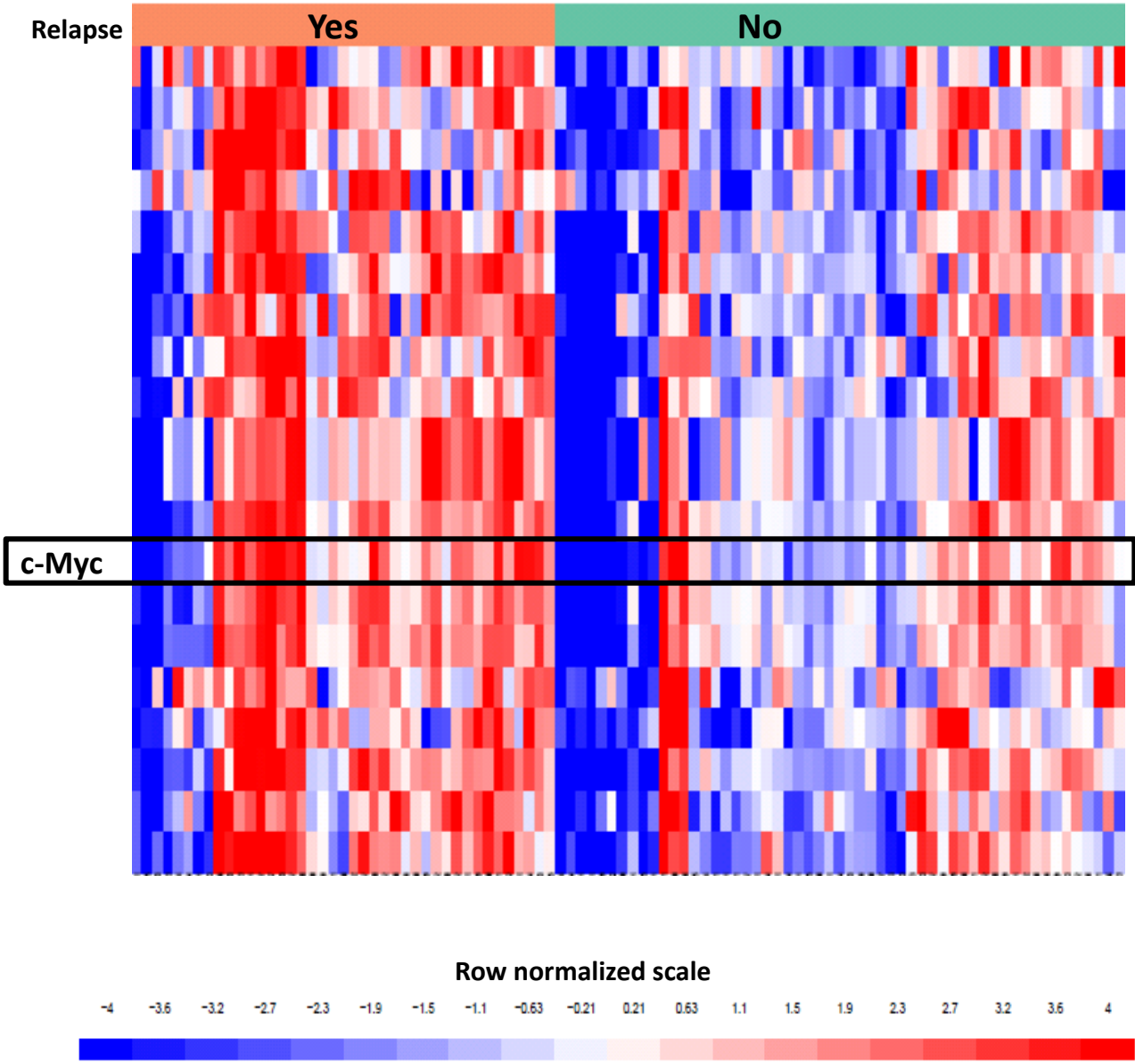


Figure S4

Disease-Subtype Dependent Expression Signatures - Training Set

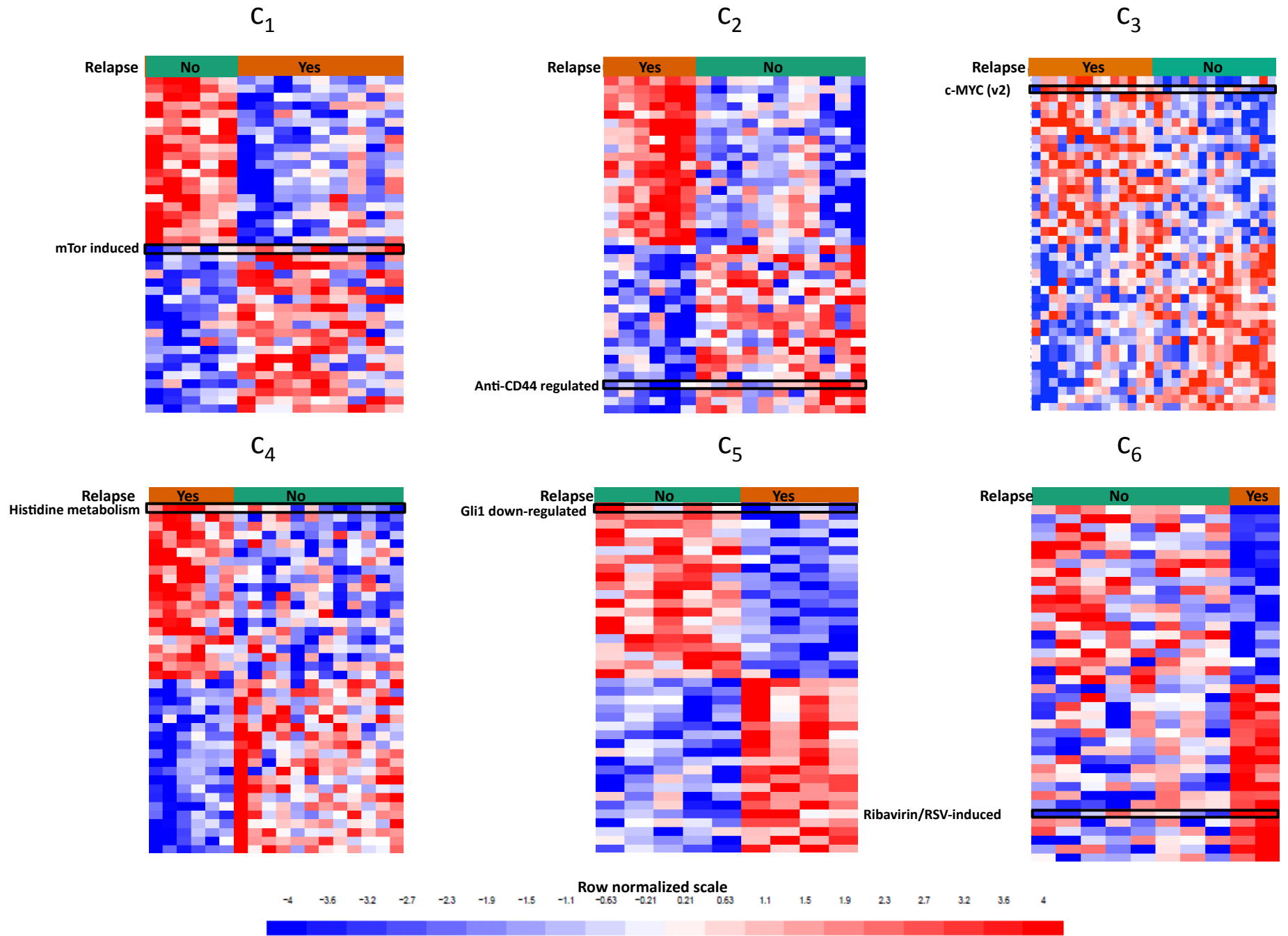


Figure S5-A

Training Set

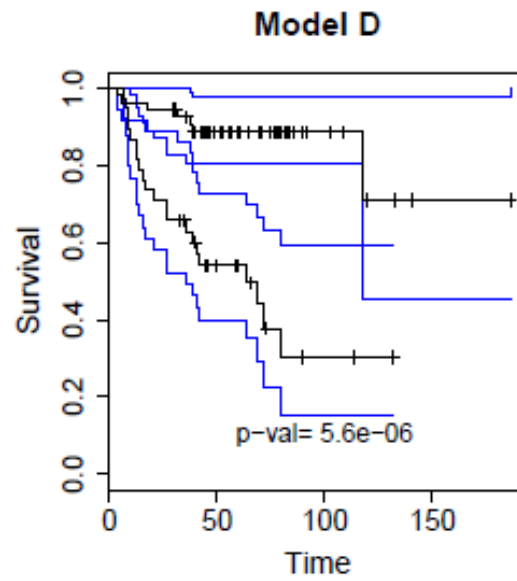
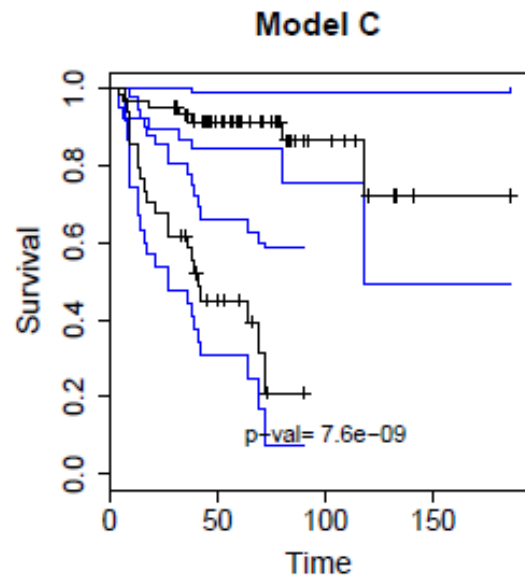
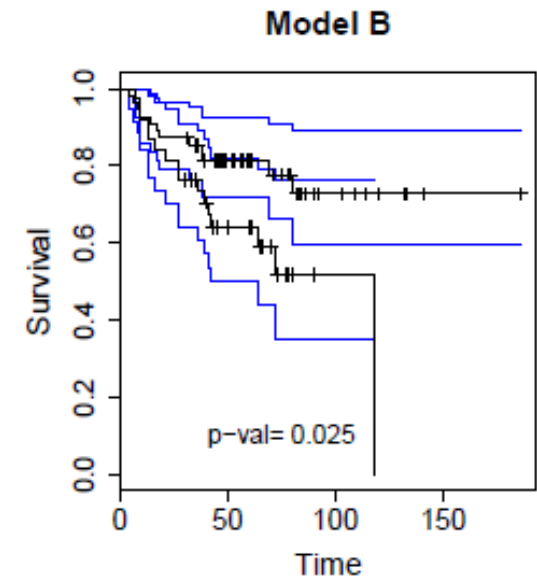
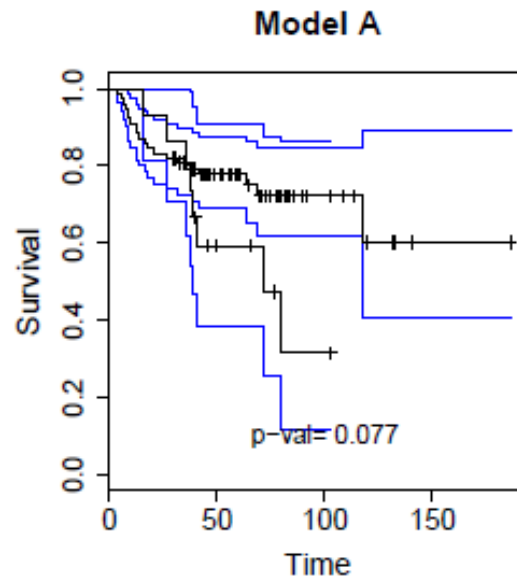
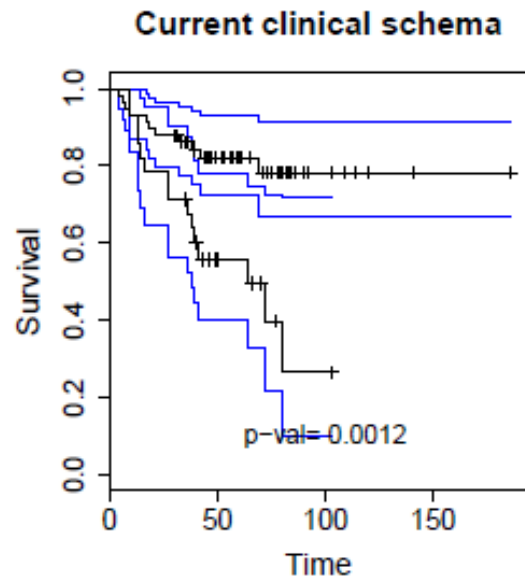


Figure S5-B

Test Set

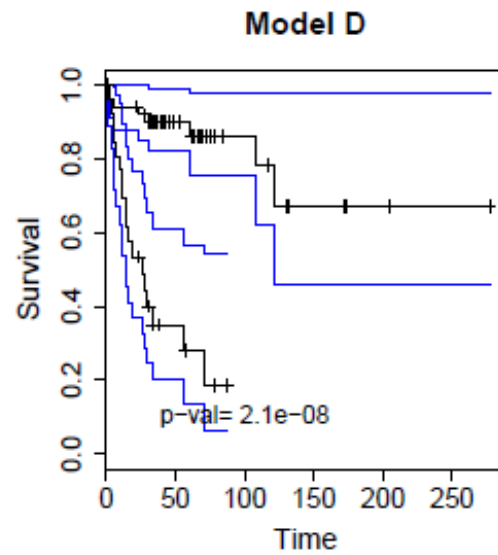
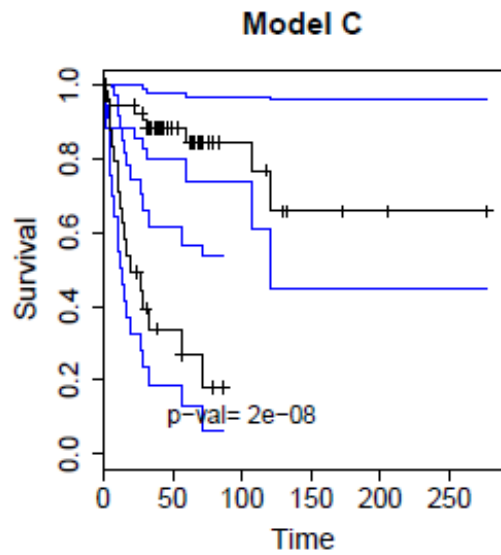
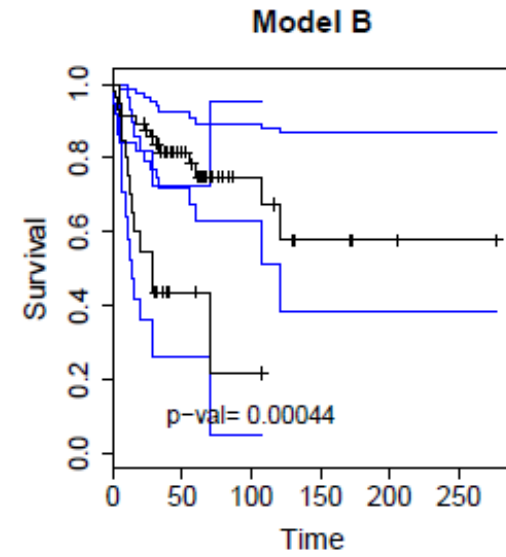
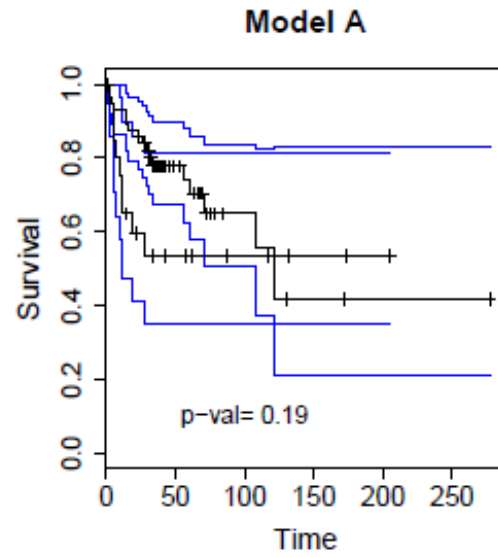
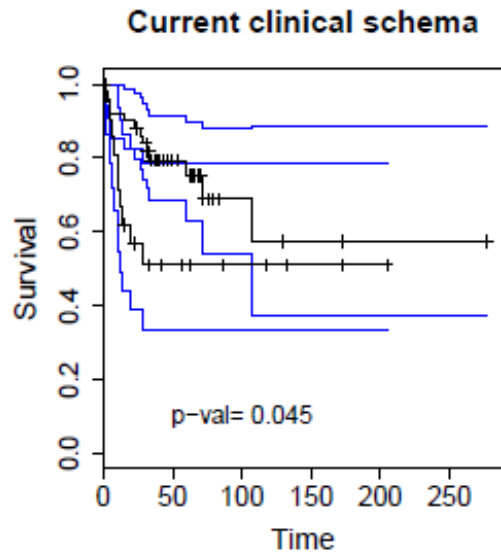
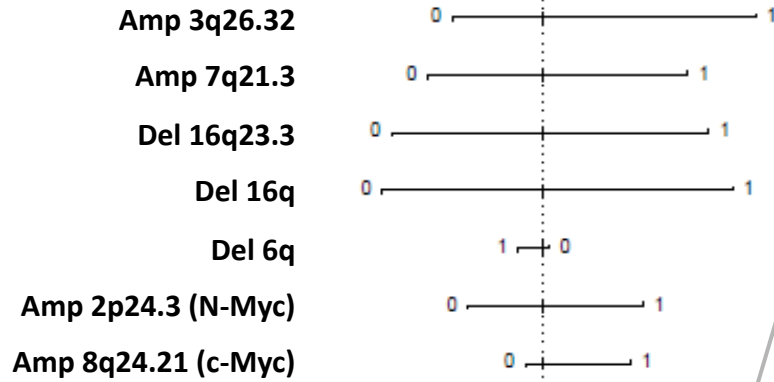
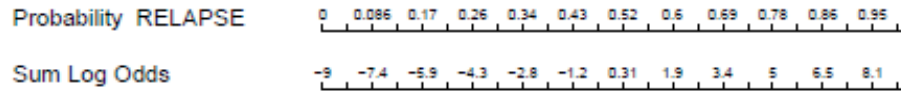


Figure S7

Full Bayesian Nomogram



Disease-Subtype Dependent Pathways

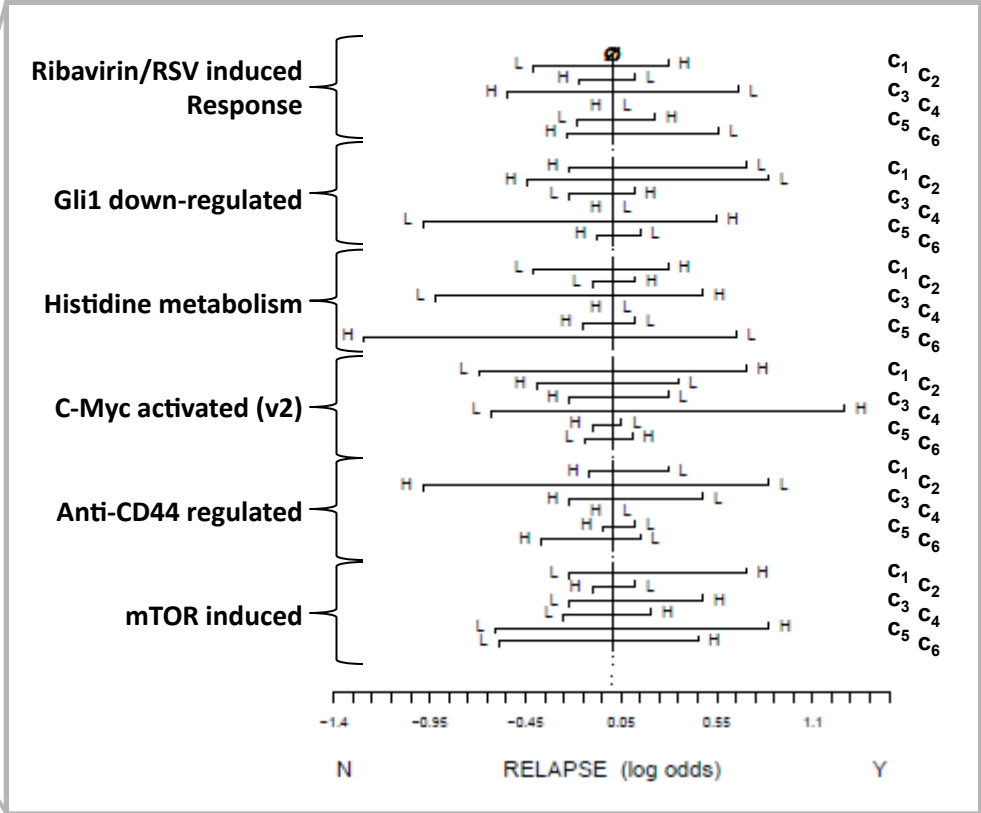
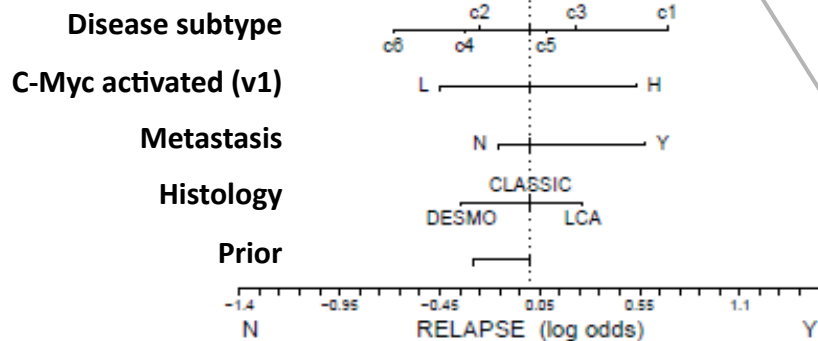


Figure S8

